Metal–Organic Frameworks

DOI: 10.1002/anie.201402951

# Perturbation of Spin Crossover Behavior by Covalent Post-Synthetic Modification of a Porous Metal–Organic Framework**

*John E. Clements, Jason R. Price, Suzanne M. Neville, and Cameron J. Kepert**

***Abstract:*** *Covalent post-synthetic modification is a versatile method for gaining high-level synthetic control over functionality within porous metal–organic frameworks and for generating new materials not accessible through one-step framework syntheses. Here we apply this topotactic synthetic approach to a porous spin crossover framework and show through detailed comparison of the structures and properties of the as-synthesised and covalently modified phases that the modification reaction proceeds quantitatively by a thermally activated single-crystal-to-single-crystal transformation to yield a material with lowered spin-switching temperature, decreased lattice cooperativity, and altered color. Structure–function relationships to emerge from this comparison show that the approach provides a new route for tuning spin crossover through control over both outer-sphere and steric interactions.*

The ability to understand and control structure and properties is a key challenge in the pursuit of multifunctional materials. One broad class of such materials, metal–organic frameworks (MOFs), are of great interest because of their facile syntheses, versatile building units, and demonstrated potential for applications that exploit their porosity and impressive capacity, selectivity, and response to guest adsorption.[1,2] While considerable progress has been achieved in synthetic control and in the development of structure–property understandings, important synthetic challenges remain in incorporating components with desired functionality into target framework topologies. One approach towards overcoming these challenges is to exploit post-synthetic modification (PSM), which uses photochemical, thermal, and synthetic transformations to obtain functionalized linkers or targeted topologies in materials that cannot be obtained readily in one synthetic step.[3] Notably, this strategy has been applied successfully to enhance porosity by inhibition of framework interpenetration in the material $[Zn_4O(L)_3]$, L = dimethyl 2-aminobiphenyl-4,4′-dicarboxylate,[4] and to access new metastable framework phases through exchanging organic linkages and metal sites post-synthetically in, for example, MIL-53 and UiO-66.[5]

An interesting subclass of porous MOFs are those that exhibit spin crossover (SCO), a phenomenon that occurs in certain $d^4$–$d^7$ transition-metal complexes in which high-spin (HS) and low-spin (LS) states can be accessed within the one material by external perturbation (e.g., temperature, pressure, light).[6] When this property is incorporated into porous MOFs, emergent behaviors such as guest-sensing are observed that exploit the interplay between the magnetic switching and host–guest processes. A number of notable examples of guest-active SCO frameworks have emerged recently,[2,7,8] and include the 2D SCO framework $[Fe_2(trans\text{-}4,4'\text{-azopyridine})_4(NCS)_4]\cdot(guest)$ (SCOF-1), which acts as a molecular "on"/"off" sensor in response to guest adsorption/desorption,[2] and the Hofmann system $[Fe^{II}(L)M^{II}(CN)_4]\cdot(guest)$ (L = pyrazine, $M^{II}$ = Ni, Pd, Pt), which displays both guest-exchange-induced SCO changes and SCO-induced changes to host–guest properties.[8]

In seeking control over structure and resulting function in SCO frameworks, PSM is an attractive strategy as it provides a method for varying host–guest effects and composition/geometry. Current such approaches include guest exchange,[2,7,8] redox intercalation,[9] and covalent guest modification.[10] Here we extend this general strategy to include covalent PSM of the SCO framework, by incorporation of an organic linker, bipytz, that readily undergoes an inverse-electron-demand Diels–Alder reaction[11] into a new 3D Hofmann-type SCO framework, $[Fe(bipytz)(Au(CN)_2)_2]$ (**1**; Figure 1). We show that the PSM reaction proceeds quantitatively by a single-crystal-to-single-crystal transformation to produce a closely related phase, $[Fe(bipydz)(Au(CN)_2)_2]$ (**2**), that exhibits markedly different SCO properties.

Bipytz was synthesized as per literature methods[12] and **1** was formed as red plates by slow diffusion of

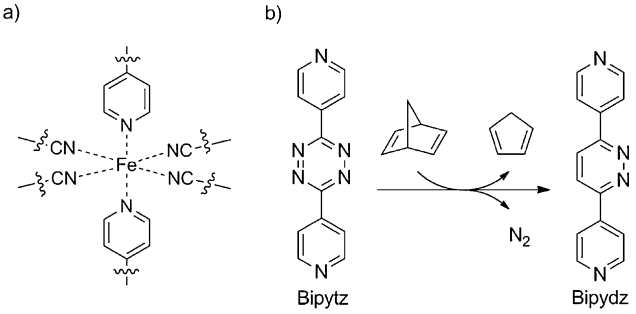


***Figure 1.*** a) General coordination sphere of Hofmann-type framework materials. b) Inverse-electron-demand Diels–Alder reaction of 3,6-bis(4-pyridyl)-1,2,4,5-tetrazine (bipytz) with 2,5-norbornadiene to form 3,6-bis(4-pyridyl)-1,2-diazine (bipydz).

[*] J. E. Clements, Dr. J. R. Price, Dr. S. M. Neville, Prof. C. J. Kepert
School of Chemistry, University of Sydney
Sydney, NSW 2006 (Australia)
E-mail: c.kepert@chem.usyd.edu.au

[**] This work was supported by research and fellowship funding from the Australian Research Council (C.J.K.) and a World Scholar Award (J.E.C.). We thank mass spectrometry service of The University of Sydney for assistance.

Supporting information for this article is available on the WWW under http://dx.doi.org/10.1002/anie.201402951.

  

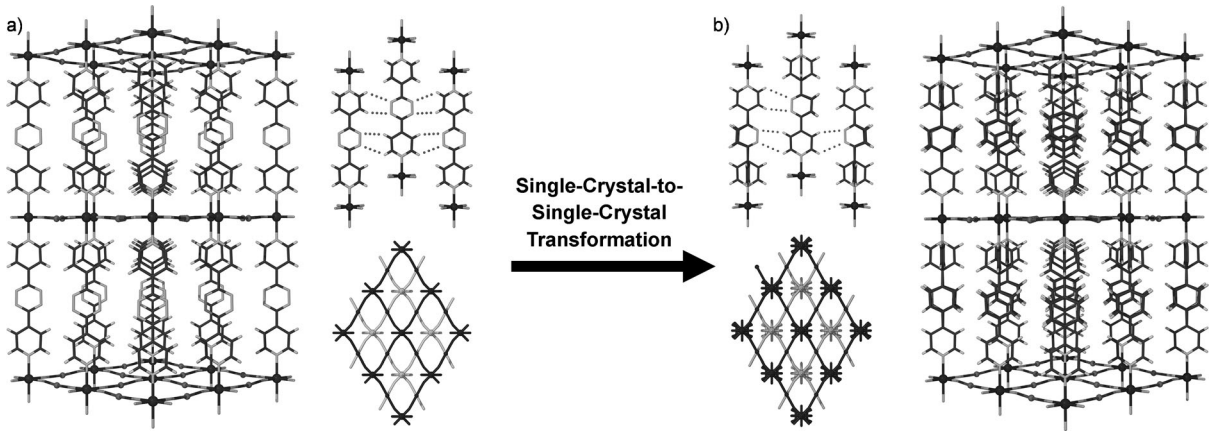


***Figure 2.*** a) Structural representations of **1**: perspective view down the *b* axis with solvent and interpenetration removed for clarity (left); C–H···N interactions between bipytz ligands across the interpenetrating nets (upper right); and view down the *c* axis with the two interpenetrating nets shaded differently (lower right). b) Corresponding structural representations of **2**, showing the subtle rotation and introduction of bipydz pillar ligand disorder with conversion of the tetrazine moiety to diazine (seen both in the four-fold disorder of the central ring and two-fold disorder of one of the pyridyl groups), and the associated disruption of ligand–ligand hydrogen bonding between interpenetrating nets.

$Fe(ClO_4)_2{\cdot}x\,H_2O$, $KAu(CN)_2$, and bipytz in ethanol. Analysis by single-crystal X-ray diffraction revealed a 3D interpenetrated extended Hofmann-type framework (see Figure 2a). The octahedral $Fe^{II}$ centers are bridged equatorially by four linear $[Au(CN)_2]^-$ linkers within the *ab* plane, with bipytz units pillaring the layers along the *c* axis through the axial sites. Interpenetration occurs such the nets are evenly spaced within *ab* and have *c*-axis separations relative to aurophilic interactions between them. The interpenetration is stabilized further by a network of host–host C–H···N hydrogen bonds between the nitrogen atoms on the bipytz tetrazine ring and hydrogen atoms on the adjacent bipytz pyridyl rings (see Figure 2a). The distances are similar to those reported for the free ligand,[13] suggesting that the framework flexes in *a* and *b* to optimize these interactions. Despite the interpenetration, the framework houses large solvent-accessible channels along the *a* axis, of dimension $8\times12$ Å.

Single-crystal diffraction data were collected at 300 and 100 K, constituting the HS and LS phases, respectively. Typically for SCO in $Fe^{II}$, two characteristic structural changes are observed upon transition from HS to LS: the average $Fe^{II}$ bond lengths ($\langle d(\text{Fe-N})\rangle$) contract by approximately 0.2 Å and the *cis* N-Fe-N angles approach 90° to form a more regular octahedron. In **1**, $\langle d(\text{Fe-N})\rangle$ contracts as expected (2.16 Å (HS); 1.95 Å (LS)) but the octahedron becomes less regular (sum of the deviation of the twelve *cis* angles from 90°, Σ: 10.16° (HS); 15.54° (LS)). We attribute this increase to an interplay between SCO and the network of intermolecular interactions which expand and contract in different ways. For example, the aurophilic interactions between dicyanide linkers shorten upon transition to LS (Au···Au: 3.275(1) Å (HS); 3.240(1) Å (LS)), whereas the host–host interactions involving the tetrazine ligand lengthen in the LS state (C···N: 3.73(2) Å, 3.64(2) Å (HS); 3.77(1) Å, 3.70(1) Å (LS)).

Magnetic susceptibility measurements on **1** reveal complete SCO with thermal hysteresis (Figure 3a). The $\chi_M T$ value changes from approximately 3.3 $cm^{-1}Kmol^{-1}$ at 290 K (typical of HS $Fe^{II}$) to 0.01 $cm^{-1}Kmol^{-1}$ at 250 K (typical of LS $Fe^{II}$). The transition between states is abrupt and has a 4 K hysteresis ($T_{1/2}\uparrow = 277$ K, $T_{1/2}\downarrow = 273$ K). Ambient temperature SCO transitions of this abrupt nature are relatively uncommon and can be attributed here to a relatively strong

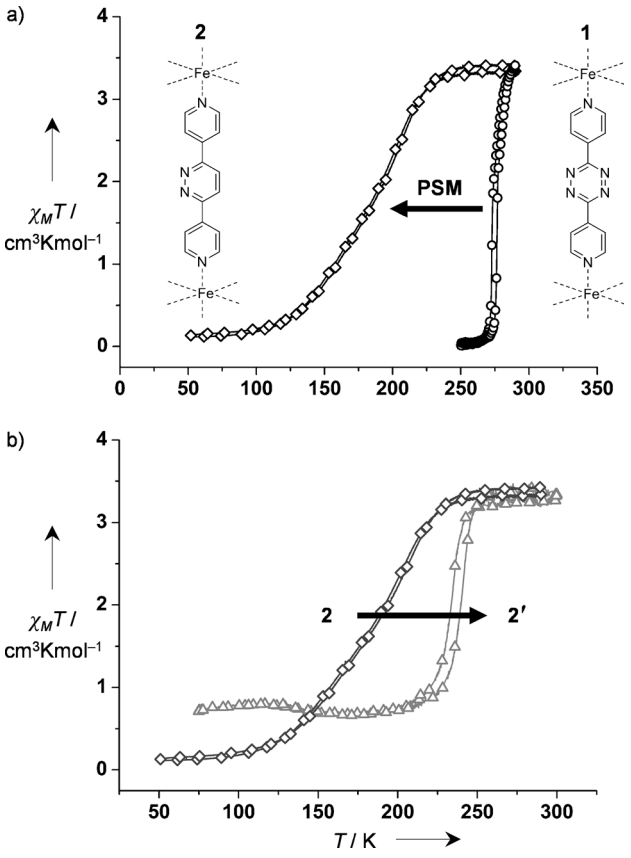


***Figure 3.*** a) Magnetic susceptibility data for **1** (○) and post-synthetically modified **2** (◇). b) The effect of guest exchange on the PSM phase: **2** (2,5-norbornadiene; ◇) and **2′** (ethanol; △).

ligand field coupled with a highly cooperative framework lattice that combines intraframework connectivity with interframework hydrogen bonding and aurophilic interactions.

Post-synthetic modification of **1** to yield **2** was performed using a method adapted from that of free bipytz in which bulk samples of **1** were heated in an excess of 2,5-norbornadiene in a sealed vessel. Washing of **2** with ethanol to remove the 2,5-norbornadiene guests led to a separate, guest-exchanged PSM phase, **2′**. The extent of conversion was confirmed to be high (>95%) through NMR analysis of the digestion products of **2**, from which no bipytz was detected (see Figure S11 in the Supporting Information). The PSM process was observed directly through a color change from purple to yellow, corresponding to the bipytz pillars in the framework converting to bipydz. Tetrazines typically display intense coloration (in this case purple) because of their low-lying π* orbital, with $n\rightarrow\pi^*$ electronic transitions being observed in the visible region.[14] We observe white coloration of bipydz but colors such as yellow, orange, and brown have been reported for substituted diazines.[15] Solid-state diffuse reflectance was thus an effective and highly convenient means to monitor the progressive conversion. As **1** reacts to form **2**, a sharp increase in reflectance below 400 nm is seen, coupled with a decrease in intensity and a shift of the main reflectance peak from 530 to 455 nm (see Figure 4a). In contrast, only minimal changes occur in the power X-ray diffraction patterns upon topotactic conversion, with the absence of impurity peaks in all patterns further confirming that the PSM process occurs cleanly (Figure 4b).

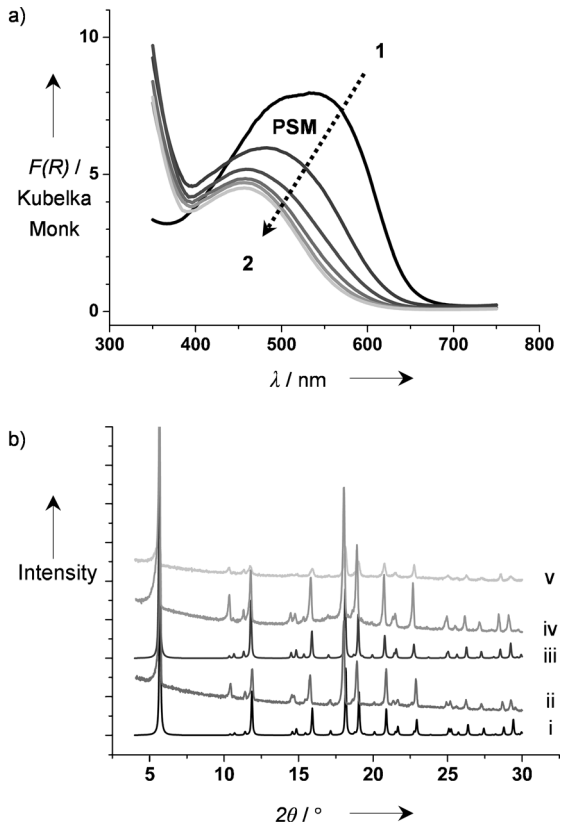


***Figure 4.*** a) Diffuse reflectance spectra for the reaction of **1** to form **2**; initial measurement after addition of 2,5-norbornadiene and subsequent spectra collected after 5, 10, 15, and 20 minutes. b) PXRD patterns of **1** (i, simulated; ii, experimental), **2** (iii, simulated; iv, experimental), and **2′** (v, experimental).

For detailed structural comparison with **1**, single-crystal structural data were collected on **2**, revealing the overall same Hofmann-type 3D interpenetrated topology observed in **1**. Indeed, the unit cell dimensions are closely comparable and the crystal symmetry (space group *Cmma*) is retained. A key consequence of the conversion of the tetrazine moiety to diazine is a decrease in the number of ligand nitrogen atoms available for host–host interactions, thereby halving the number of interframework C–H···N contacts. Accordingly, the principal structural difference between **1** and **2** is that the diazine unit of the bipydz ligand, rather than being coplanar, is now rotated by approximately 20° with respect to the pyridyl units because of the disruption of interframework hydrogen bonding and to the introduction of both interframework and intraligand H···H repulsion (see Figure 2b and Table S1). The ligand lies on a *mm2* symmetry axis and thus there is four-fold disorder of this rotation; no structural ordering of the diazine ring is evident, suggesting there is no regioselectivity in the PSM process, although short-range and/or low-dimensional ligand ordering may be present. A further difference between **1** and **2** is the introduction of subtle disorder of the pyridyl ring that is not "locked" by the hydrogen-bonding interactions, such that there are now two local orientations, one in-plane with the other pyridyl ring (ca. 80% occupancy) and the other perpendicular to it (ca. 20%). The aurophilic interactions present in **1** are retained in **2**. Not only does this topotactic modification proceed by a single-crystal-to-single-crystal transformation but no loss of crystallinity is observed; in contrast, many materials are known to degrade upon lesser changes (e.g., SCO, guest exchange).[16]

As with **1**, single-crystal diffraction data were collected on **2** in the HS and LS states, at 290 and 90 K respectively. The variation in $Fe^{II}$ coordination environment with spin state is similar to that observed in **1** ($\langle d(\text{Fe-N})\rangle$: 2.17 Å (HS), 1.98 Å (LS); $\Sigma$: 12.00° (HS), 13.75° (LS)); again, the increased distortion of the $FeN_6$ octahedron at low temperature arises with competition between ligand field stabilization and interframework interaction energies. The Au···Au distance is shorter than in **1** and, as before, contracts upon cooling (Au···Au: 3.167(1) Å (HS), 3.098(1) Å (LS)). In contrast, the host–host C–H···N hydrogen bond distances are longer in **2** than **1** and lengthen to a lesser extent on cooling (C···N: 3.87(3) cf. 3.78(3) Å (HS); 4.06(5) cf. 4.01(6) Å (LS) for **2** cf. **1**).

As an initial view of the spin switching properties, immersion in liquid nitrogen revealed that **2** changes from yellow to red, whereas **1** does not undergo dramatic changes in chromism despite its SCO because of the overlap of the bipytz ligand $n\rightarrow\pi^*$ and LS $Fe^{II}$ d–d bands. Magnetic susceptibility data for **2** show a complete SCO with $\chi_M T$ varying from approximately 3.3 $cm^{-1}Kmol^{-1}$ at 290 K to 0.1 $cm^{-1}Kmol^{-1}$ at 50 K (Figure 3a). The similarity in SCO completeness to that of **1** is noteworthy as PSM might be expected to introduce structural defects, which most commonly results in increased HS residuals and more gradual

  

SCO.[17] This result complements the structural data in indicating that the PSM process yields a very high quality sample. In contrast, despite the retention of a clean PXRD pattern (Figure 4b), some degree of framework degradation and/or increased local disorder is suggested by the incomplete SCO observed following ethanol exchange to form **2′** (Figure 3b).

The SCO behavior of **2** differs from that of **1** in three ways: it is less abrupt; occurs at lower temperature ($T_{1/2}$ = 178 K); and is not detectably hysteretic. These changes can be attributed to a number of different influences, both electronic and structural. The lower $T_{1/2}$ value suggests a reduced ligand field following conversion of the tetrazine to a diazine pillar. Changes here involve a loss of withdrawing character from the tetrazine as the more electron-rich diazine is formed and the introduction of ring torsion in bipydz; the former would likely increase the electron-donating ability of the pillaring ligand, but when the loss of intramolecular orbital overlap is also considered, coupled with the pyridyl ring disorder, the possible decrease in pillar ligand field may be accredited to a loss in π-accepting ability. Likely to be more dominant in effect, as evidenced by the subsequent increase in SCO temperature following exchange of the 2,5-norbornadiene guests with ethanol (Figure 3b), are various steric influences. The lower $T_{1/2}$ in **2** is broadly consistent with the lower ligand field implied by the greater octahedral distortion in the HS state and more distorted cyanide coordination (Fe-NC angle: HS 165.2 cf. 165.8°; LS 170.3 cf. 170.6° for **1** cf. **2**), although somewhat conflicting with the lesser octahedral distortion observed in the LS state of **2**. Host–host and host–guest interactions are also likely to have a direct influence on SCO temperature. Notably, the C–H···N interactions are shorter and twice as prevalent in **1**, yielding a greater compressive influence on the structure and therefore being likely to lead to a greater stabilization of the LS state. Furthermore, the presence of the larger, 2,5-norbornadiene guest in **2** is likely to destabilize the LS state through an internal guest pressure effect in which lower temperatures are required for pore compression associated with the HS-to-LS conversion; the subsequent increase in SCO temperature following ethanol exchange (Figure 3b) is consistent with this.

The gradual nature of the SCO in **2** compared to that of **1**, a property that is replicated in variable temperature single-crystal diffraction data and so does not reflect sample broadening (see Figure S6), can be attributed principally to the presence of 2,5-norbornadiene rather than ethanol within the pores of **2**; SCO materials adsorbed with larger guests tend to have more gradual transitions because of their exertion of an internal pressure, preventing more cooperative structural contraction to LS.[8] Ethanol exchange leads to a pronounced sharpening of the transition in **2′** and to a restoration of thermal hysteretic behavior ($T_{1/2}\uparrow$ = 240 K, $T_{1/2}\downarrow$ = 233 K; Figure 3b), confirming that the gradual nature of SCO in **2** arises from a guest-induced effect. The incomplete restoration of transition abruptness in **2′** can be tentatively attributed to the decreased lattice cooperativity resulting from the halving in number of interframework hydrogen-bonding interactions; it has been recognized previously in other systems that intramolecular interactions (hydrogen bonding and π-stacking) can influence the propagation of SCO through a lattice.[18] The decreased SCO abruptness of **2′** over that of **1** also likely results to some degree from local structural heterogeneity associated with, for example, the bipydz ligand disorder.

To conclude, we show that a robust metal–organic framework that exhibits abrupt SCO can be modified under mild conditions by an inverse-electron-demand Diels–Alder reaction to yield a closely related crystalline phase with markedly different electronic switching properties. The differences observed can be traced to a range of structural perturbations that arise with the covalent modification, the most notable being subtle changes in framework geometry and a decrease in the degree of lattice cooperativity associated with a halving in the number of interframework hydrogen bonds. Interestingly, we find that the structure and magnetic characteristics of the PSM material are not achievable through one-step synthesis using the ex situ pre-functionalized bipydz ligand, with this approach producing instead a different (but related) structure with an interesting multi-stepped SCO behavior that will be described in a future report. Overall, we demonstrate the potency of covalent PSM as a means to perturb and, in principle, introduce increased structural complexity into SCO systems, thereby expanding the scope of this class of multifunctional materials through the opportunity to incorporate specific functional sites. Further, this topotactic approach promises a new method to control nanostructure (e.g., core–shell structure) within SCO crystallites. From a quite separate viewpoint, there is potential for SCO centers embedded within reactive frameworks to act as sensors for covalent reactions—a new and potentially highly selective route to guest-sensing.

## Experimental Section

Crystals of $[Fe(bipytz)(Au(CN)_2)_2]\cdot x\,EtOH$ (**1**) were obtained by the slow diffusion of ethanol solutions of bipytz (9 mg, 0.038 mmol), $KAu(CN)_2$ (22 mg, 0.076 mmol), and $Fe(ClO_4)_2\cdot x\,H_2O$ (10 mg, 0.039 mmol). Red plates of **1** formed over several weeks. Bulk samples were prepared with faster addition rates and purity was confirmed by PXRD analysis. All samples were washed with ethanol prior to structural and physical measurement.

Samples of **2** were prepared by heating a mixture of **1** and excess 2,5-norbornadiene to 50 °C for 35 min then cooling in an ice bath. Identity was confirmed by PXRD analysis and by NMR analysis of the framework digestion products. For SCXRD analysis, red plates of **1** (ca. 1 mg) were placed in a glass tube, the mother liquor decanted, and 2,5-norbornadiene (0.25 mL) was added. The tube was flame-sealed and heated at 65 °C for 24 h, producing yellow plates of **2**.

CCDC 989411, 989412, 989413, 989414 contain the supplementary crystallographic data for this paper. These data can be obtained free of charge from The Cambridge Crystallographic Data Centre via www.ccdc.cam.ac.uk/data_request/cif.

Received: March 3, 2014
Revised: June 26, 2014
Published online: July 24, 2014

**Keywords:** host–guest systems · metal–organic frameworks · microporous materials · supramolecular chemistry

  

[1] a) T. M. McDonald, D. M. D'Alessandro, R. Krishna, J. R. Long, *Chem. Sci.* **2011**, *2*, 2022 – 2028; b) S. Horike, Y. Inubushi, T. Hori, T. Fukushima, S. Kitagawa, *Chem. Sci.* **2012**, *3*, 116 – 120; c) N. R. Champness, *Dalton Trans.* **2011**, *40*, 10311 – 10315.
[2] G. J. Halder, C. J. Kepert, B. Moubaraki, K. S. Murray, J. D. Cashion, *Science* **2002**, *298*, 1762 – 1765.
[3] S. M. Cohen, *Chem. Sci.* **2010**, *1*, 32 – 36.
[4] R. K. Deshpande, J. L. Minnaar, S. G. Telfer, *Angew. Chem.* **2010**, *122*, 4702 – 4706; *Angew. Chem. Int. Ed.* **2010**, *49*, 4598 – 4602.
[5] M. Kim, J. F. Cahill, H. H. Fei, K. A. Prather, S. M. Cohen, *J. Am. Chem. Soc.* **2012**, *134*, 18082 – 18088.
[6] P. Gütlich, A. B. Gaspar, Y. Garcia, *Beilstein J. Org. Chem.* **2013**, *9*, 342 – 391.
[7] a) K. Yoshida, D. Akahoshi, T. Kawasaki, T. Saito, T. Kitazawa, *Polyhedron* **2013**, *32*, 252 – 256; b) E. Coronado, M. Gimenez-Marques, G. M. Espallargas, F. Rey, I. J. Vitorica-Yrezabal, *J. Am. Chem. Soc.* **2013**, *135*, 15986 – 15989; c) N. F. Sciortino, K. R. Scherl-Gruenwald, G. Chastanet, G. J. Halder, K. W. Chapman, J.-F. Létard, C. J. Kepert, *Angew. Chem.* **2012**, *124*, 10301 – 10305; *Angew. Chem. Int. Ed.* **2012**, *51*, 10154 – 10158; d) F. J. Muñoz Lara, A. B. Gaspar, D. Aravena, E. Ruiz, M. C. Muñoz, M. Ohba, R. Ohtani, S. Kitagawa, J. A. Real, *Chem. Commun.* **2012**, *48*, 4686 – 4688; e) C. Bartual-Murgui, N. A. Ortega-Villar, H. J. Shepherd, M. C. Muñoz, L. Salmon, G. Molnar, A. Bousseksou, J. A. Real, *J. Mater. Chem.* **2011**, *21*, 7217 – 7222; f) M. Ohba, K. Yoneda, G. Agustí, M. C. Muñoz, A. B. Gaspar, J. A. Real, M. Yamasaki, H. Ando, Y. Nakao, S. Sakaki, S. Kitagawa, *Angew. Chem.* **2009**, *121*, 4861 – 4865; *Angew. Chem. Int. Ed.* **2009**, *48*, 4767 – 4771; g) S. M. Neville, G. J. Halder, K. W. Chapman, M. B. Duriska, B. Moubaraki, K. S. Murray, C. J. Kepert, *J. Am. Chem. Soc.* **2009**, *131*, 12106 – 12108; h) S. M. Neville, B. A. Leita, G. J. Halder, C. J. Kepert, B. Moubaraki, J.-F. Létard, K. S. Murray, *Chem. Eur. J.* **2008**, *14*, 10123 – 10133; i) S. M. Neville, G. J. Halder, K. W. Chapman, M. B. Duriska, P. D. Southon, J. D. Cashion, J.-F. Létard, B. Moubaraki, K. S. Murray, C. J. Kepert, *J. Am. Chem. Soc.* **2008**, *130*, 2869 – 2876; j) G. J. Halder, K. W. Chapman, S. M. Neville, B. Moubaraki, K. S. Murray, J.-F. Létard, C. J. Kepert, *J. Am. Chem. Soc.* **2008**, *130*, 17552 – 17562; k) S. M. Neville, B. Moubaraki, K. S. Murray, C. J. Kepert, *Angew. Chem.* **2007**, *119*, 2105 – 2108; *Angew. Chem. Int. Ed.* **2007**, *46*, 2059 – 2062; l) B. A. Leita, S. M. Neville, G. J. Halder, B. Moubaraki, C. J. Kepert, J.-F. Létard, K. S. Murray, *Inorg. Chem.* **2007**, *46*, 8784 – 8795; m) V. Niel, A. L. Thompson, M. C. Muñoz, A. Galet, A. S. E. Goeta, J. A. Real, *Angew. Chem.* **2003**, *115*, 3890 – 3893; *Angew. Chem. Int. Ed.* **2003**, *42*, 3760 – 3763; n) R. J. Wei, J. Tao, R. B. Huang, L. S. Zheng, *Inorg. Chem.* **2011**, *50*, 8553 – 8564.
[8] P. D. Southon, L. Liu, E. A. Fellows, D. J. Price, G. J. Halder, K. W. Chapman, B. Moubaraki, K. S. Murray, J.-F. Létard, C. J. Kepert, *J. Am. Chem. Soc.* **2009**, *131*, 10998 – 11009.
[9] R. Ohtani, K. Yoneda, S. Furukawa, N. Horike, S. Kitagawa, A. B. Gaspar, M. C. Muñoz, J. A. Real, M. Ohba, *J. Am. Chem. Soc.* **2011**, *133*, 8600 – 8605.
[10] X. Bao, H. J. Shepherd, L. Salmon, G. Molnar, M. L. Tong, A. Bousseksou, *Angew. Chem.* **2013**, *125*, 1236 – 1240; *Angew. Chem. Int. Ed.* **2013**, *52*, 1198 – 1202.
[11] C. F. Hansell, P. Espeel, M. M. Stamenovic, I. A. Barker, A. P. Dove, F. E. Du Prez, R. K. O'Reilly, *J. Am. Chem. Soc.* **2011**, *133*, 13828 – 13831.
[12] P. H. Dinolfo, M. E. Williams, C. L. Stern, J. T. Hupp, *J. Am. Chem. Soc.* **2004**, *126*, 12989 – 13001.
[13] N. S. Oxtoby, A. J. Blake, N. R. Champness, C. Wilson, *CrystEngComm* **2003**, *5*, 82 – 86.
[14] W. Kaim, *Coord. Chem. Rev.* **2002**, *230*, 127 – 139.
[15] E. C. Constable, C. E. Housecroft, M. Neuburger, S. Reymann, S. Schaffner, *Eur. J. Org. Chem.* **2008**, 1597 – 1607.
[16] a) S. Hayami, Z. Gu, Y. Einaga, Y. Kobayasi, Y. Ishikawa, Y. Yamada, A. Fujishima, O. Sato, *Inorg. Chem.* **2001**, *40*, 3240 – 3242; b) S. L. James, *Chem. Soc. Rev.* **2003**, *32*, 276 – 288.
[17] M. S. Haddad, W. D. Federer, M. W. Lynch, D. N. Hendrickson, *Inorg. Chem.* **1981**, *20*, 131 – 139.
[18] a) M. Marchivie, P. Guionneau, J.-F. Létard, D. Chasseau, *Acta Crystallogr. Sect. B* **2003**, *59*, 479 – 486; b) M. A. Halcrow, *Chem. Soc. Rev.* **2011**, *40*, 4119 – 4142.

  